Fault detection combining adaptive degrees of freedom χ2-statistics and interval approach for nonlinear systems

Quoc Hung Lu, Soheib Fergani, Carine Jauberthie

Fault detection combining adaptive degrees of freedom χ^2-statistics and interval approach for nonlinear systems

Quoc Hung Lu * **Soheib Fergani** * **Carine Jauberthie** *

* *LAAS-CNRS, 7 avenue du Colonel Roche, 31400 Toulouse, France (e-mail: qhlu@laas.fr, sfergani@laas.fr, cjaubert@laas.fr).*

Abstract: An enlargement of the *Adaptive degrees of freedom χ^2-statistics* (ADFC) method to fault detection for nonlinear systems with mixed uncertainties (stochastic and bounded uncertainties) is presented in this paper. The ADFC approach, primarily developped for fault detection in case of linear systems, is then combined with the *Reinforced likelihood box particle filter* (RLBPF). A *residual generator* is used, followed by the *adaptive amplifier coefficient* (a.a.c.) concept in the *decision making* stage. Then, the proposed approach is applied to a nonlinear Magneto-Rheological damper model to illustrate the efficiency of the method.

Keywords: Adaptive Innovation-based method, Fault diagnosis, Adaptive amplifier coefficient, Automotive quarter model.

1. INTRODUCTION

In modern control system, many important issues are required to be solved such as the availability, cost efficiency, reliability, operating safety, environmental protection,... Therefore, *fault diagnosis* becomes indispensable and one of the main solutions for these requirements. A fault must be diagnosed as early as possible, even if it may be tolerable, to prevent any serious consequence. The fault diagnosis consists in three tasks: *fault detection* (FD), *fault isolation* and *fault estimation* (or fault identification), in which FD is the first stage and building block of any further task. For all the above reasons, this paper is focusing on the developement of a reliable FD strategy.

Model-based FD approach applied to dynamical systems using *analytical redundancy* is widely used. It consists in two stages: *residual generation* and *residual evaluation* or *decision making*. The residual is normally a difference between a measured signal and an estimate of the later. It should be zero-valued in the *fault-free* case and diverge from zero in the *faulty* case. In the second stage, the residual (or its transformation via a function) is compared to a *constant threshold* or an *adaptive threshold* depending on the fault detection method. Especially, using *observer-based* concept, a filter or an observer is the core of the residual generator which provides the estimate quantity of interest to deduce the residual. This is the structure of the FD method proposed in the paper (Fig.1). The most advantage of this structure is that it can easily combine filter/observer and decision making method (pre-existent or to be developed) for adapting to various contexts and purposes.

The challenge of the present work is twofold: the non linearity of the system and the mixed uncertainties context (bounded and stochastic uncertainties). Indeed, in the literature, most of researches about FD are devoted to linear

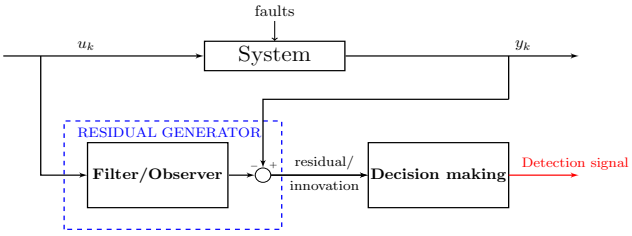

Fig. 1. General structure of observer-based Fault detection.

system while fewer articles provide solution for non linear counterpart. Nonlinear systems are usually assumed to be *smooth* "enough" with mild conditions for a nice linearization, then techniques for the linear case can be applied. For instance, the Standard Kalman Filter (SKF)(Kalman, 1960) and its extensions (included *Extended Kalman Filter* (EKF), *Unscented Kalman Filter* (UKF), *Robust Kalman fitering*, *Interval Kalman Filter* (IKF), *Minimum Upper Bound of Variance Interval Kalman Filter* (UBIKF), *Optimal upper bounded Interval Kalman Filter* (OUBIKF)) have been applied in residual generators of different FD schemes/methods. We refer to Zhong et al. (2018) which provides a survey on model-based fault diagnosis for *linear discrete time-varying* (LTV) systems with useful references concerning FD using SKF, EKF and UKF. Otherwise, Xiong et al. (2013) proposed FD method using IKF, Tran (2017) with FD using UBIKF, Lu et al. (2021) with FD based on OUBIKF, while output observer (non interval case) for FD in linear systems can be found in Mohamadi et al. (2016). Furthermore, also for linear system, *set-membership* methods in fault diagnosis are concerned in Puig (2010) while *interval observer* approach for FD is investigated, for instance, in Raka and Combastel (2013); Chevet et al. (2021). Some of these works (Xiong et al., 2013; Tran, 2017; Lu et al., 2021) deal with mixed un-

certainties context while the remaining deal either with bounded or stochastic uncertainties only.

In the present paper, an enlargement of the *Adaptive degrees of freedom χ^2-statistics* (ADFC) method (Lu et al., 2021) to FD for non linear system is proposed. The method combines the *Reinforced likelihood box particle filter* (RLBPF) developed in Lu et al. (2022) (versus OUBIKF for linear system) together with the *adaptive amplifier coefficient* (a.a.c.) concept in the decision making stage. In doing so, the twofold challenge of the issue is met. *Interval analysis* is a primary tool for computation of the method, no strict condition is required for (non linear) dynamic functions of the system.

The paper is organized as follows. Preliminaries are provided in Section 2, including used notations and essential of interval analysis. Section 3 presents main results with the extended FD method. Simulations based on the non-linear Magneto-Rheological damper model are provided in Section 4. Finally, Section 5 provides conlusions and perspectives.

2. PRELIMINARY

2.1 Essential of interval analysis

A *real interval* $[x] = [\underline{x}, \overline{x}] = \{t \in \mathbb{R} \,|\, \underline{x} \leq t \leq \overline{x}\}$ is a *closed connected subset* of $\mathbb{R}$ and characterized by two extreme values $\underline{x} \leq \overline{x}$. A *real interval matrix* $[X] = ([x_{ij}])$ of dimension $p \times q$, also called an interval in $\mathbb{R}^{p\times q}$, is a matrix with real interval components $[x_{ij}]$, $i \in \{1, ..., p\}$, $j \in \{1, ..., q\}$. Write $X \in [X]$ to indicate a *point matrix* $X = (x_{ij})$ *belonging element-wise* to $[X]$. Define:

- $\sup([X]) \triangleq (\sup([x_{ij}])) \equiv \overline{X}$,
- $\inf([X]) \triangleq (\inf([x_{ij}])) \equiv \underline{X}$,
- $\text{mid}([X]) \triangleq (\overline{X} + \underline{X})/2$,
- $\text{rad}([X]) \triangleq (\overline{X} - \underline{X})/2$,
- $\text{width}([X]) \triangleq \overline{X} - \underline{X}$,

which are called respectively (resp.) the *largest matrix*, the *smallest matrix*, the *midpoint matrix*, the *radius matrix* and the *width matrix* of $[X]$. Define the *hull* of a closed set S and the hull of two interval $[X_1]$, $[X_2]$ of the same dimension as follows: $\text{hull}\{\emptyset\} \triangleq \emptyset$, $\text{hull}\{S\} \triangleq [\inf(S), \sup(S)]$ and $\text{hull}\{[X_1], [X_2]\} \triangleq [\inf\{\underline{X}_1, \underline{X}_2\}, \sup\{\overline{X}_1, \overline{X}_2\}]$. We also write an interval as: $[X] = [\underline{X}, \overline{X}] = \text{mid}([X]) \pm \text{rad}([X])$.

Basic interval operators $\diamond \in \{+, -, \times, \div\}$ defined in Jaulin et al. (2001) can be used to compute directly all operations $[u] \diamond [v]$ and $\alpha \diamond [u]$, for real intervals $[u]$, $[v]$ and $\alpha \in \mathbb{R}$, without any further approximation algorithm. Then, interval matrix computations are defined similarly to matrix computations using the basic operators while more general operators are constructed by means of inclusion function $[f]$ defined in Definition 1 below. In practice, the package Intlab Rump (1999) developed for Matlab (also existing in Octave and C/C++) is used for computations.

Definition 1. Let f be any function from $D \subseteq \mathbb{R}^m$ to $\mathbb{R}^n$. An *inclusion function* of f is a function $[f]$ that maps any interval $[x]$ in D to an interval $[f]([x])$ in $\mathbb{R}^n$ containing the image set $f([x])$. Symbolically,

$$[f] : [x] \mapsto [f]([x]) \supset f([x]), \forall [x] \subset D,$$

with $[f]([x])$ is an interval in $\mathbb{R}^n$. The *minimal* inclusion function of f is a function $[f]^*$ so that for every $[x] \subset D$, $[f]^*([x])$ is the smallest interval containing $f([x])$. □

If f is composed by a finite number of operators ($+$, $-$, $\times$, $\div$) and elementary functions (exp, sin, cos, $\sqrt{(.)}$, ...) then a *natural inclusion function* of f is a function $[f]$ having the same expression of the former in which point variables are replaced by corresponding interval variables while operators and functions are replaced by their interval counterpart. There is other commonly used inclusion function such as *centred inclusion function, mixed centred inclusion function, Taylor inclusion function,...* (see Jaulin et al. (2001) for more details).

2.2 Other notations

A positive semidefinite matrix X is denoted by $X \succeq 0$. Let $M, N \in \mathbb{R}^{n\times n}$, define $N \preceq M$ if $M - N \succeq 0$, M is called an *upper bound* of N and N a *lower bound* of M. Let $\emptyset \neq \Omega \subset \mathbb{R}^{n\times n}$, M is an upper bound (resp. lower bound) of Ω, denoted $\Omega \preceq M$ (resp. $M \preceq \Omega$) , if $X \preceq M$ (resp. $M \preceq X$), $\forall X \in \Omega$.

Denote also: $S_+([X]) \triangleq \{X \in [X] : X = X^T \text{ and } X \succeq 0\}$, $\mathbb{I}(x) = 1$ if the conditions x are true and $\mathbb{I}(x) = 0$ otherwise, $\text{mean}(x) = \sum_{i=1}^{n} x_i/n$, $\forall x \in \mathbb{R}^n$. The notation $p : l : q$ ($p \leq q$) is used for a range from p to q with step l. For $l = 1$, we write $p : q$. A sequence of variables can be noted interchangeably as $w_1, ..., w_k$ or $w_1 : w_k$ or $w_{1:k}$.

3. MAIN RESULTS

3.1 Model and problem formulation

Consider the following system (1) with additive measurement noises :

$$(\boldsymbol{\Sigma}) \; : \; \begin{cases} x_k = f_k(x_{k-1}, u_k, w_k) \; , \\ y_k = h_k(x_k, u_k) + v_k + f_k^s \; , \end{cases} \qquad k \in \mathbb{N}^*, \quad (1)$$

where $x_k \in \mathbb{R}^{n_x}$ and $y_k \in \mathbb{R}^{n_y}$ represent state variables and measures respectively, $u_k \in \mathbb{R}^{n_u}$ inputs, $w_k \in \mathbb{R}^{n_x}$ state disturbances/noises, $v_k \in \mathbb{R}^{n_y}$ measurement noises, $f_k^s \in \mathbb{R}^{n_y}$ additive sensor fault vectors. Each of its components corresponds to a sensor fault. Thus, the fault vector f_k^s can be of the multiple or single error type.

Assumptions (A)

(A1) Given $[x_0]$, $[u_k]$, $[w_k]$, $[y_k]$, $[\mu_k]$, f_k, h_k, $k \in \mathbb{N}^*$.

(A2) $v_k \sim \mathcal{N}(\mu_k, \Sigma_k)$ with unknown μ_k and Σ_k.

(A3) $x_0 \in [x_0]$, $u_k \in [u_k]$, $w_k \in [w_k]$, $y_k \in [y_k]$, $\mu_k \in [\mu_k]$ and $\Sigma_k \in [\Sigma_k]$.

(A4) $[\Sigma_k]$ is unknown.

Remark 2. The measurements are given as intervals $[y_k]$ due to the sensor precision. In many theoretical problems and applications, it is assumed that $\mu_k \equiv [\mu_k] \equiv 0$ for simplicity. It is natural that $[\Sigma_k]$ is unknown and the mention of this fact is necessary for the subsequent development. Assumptions (A3) are implicitly deduced that the belonging of unknown real (true) terms in their corresponding intervals are *certain*. This certainty can be understood as "*with probability 1*". System (1) with

assumptions (A) can be adapted to a wide range of applications. The system is time varying, the uncertainties come from system disturbances or measurement noises with different kinds (stochastic/bounded uncertainties). □

To evaluate the fault detection performance, four indicators are introduced. Assume that system (1) is applied for N iterations among which faults occur in a time inteinte $\mathcal{R}$ with length l ($0 \leq l \leq N$). Actually, $\mathcal{R}$ may be an interval or union of intervals but is called hereafter an *error range* for simplicity. Then, a detection signal is denoted by π_k which has values in $\{0; 1\}$. A signal $\pi_k = 1$ is called a *right detected signal* if $k \in \mathcal{R}$ and a *false detected signal* if $k \notin \mathcal{R}$. Then, the four indicators are defined as follows:

+ *Detection Rate*: $\text{DR} = \sum_{k\in\mathcal{R}} \frac{\mathbb{I}(\pi_k=1)}{l} \times 100\%$,
+ *False Alarm Rate*: $\text{FAR} = \sum_{k\notin\mathcal{R}} \frac{\mathbb{I}(\pi_k=1)}{N-l} \times 100\%$,
+ *Efficiency*: $\text{EFF} = \text{DR} - \text{FAR}$,
+ *No detection rate*: $\text{NDR} = 100\% - \text{DR}$.

3.2 Adaptive approach combining RLBPF to fault detection

In this section, the ADFC method is extended to a more general framework, including nonlinear dynamical systems. This approach has also the ability to combine with several set-membership estimation filters (w.r.t to some conditions in see Theorem 3). In the following, the proposed approach is applied with RLBPF and the extension is based on Theorem 3.

Theorem 3. Consider system ($\mathbf{\Sigma}$) with assumptions **(A)** and fault free case ($f_k^s = 0, \forall k \in \mathbb{N}^*$).
Let $r_k = y_k - h_k(x_k, u_k) - \mu_k$ be the residual, $[\hat{x}_{k|k}]$ be interval estimates of an interval filter and

$$[\hat{x}_{k+1|k}] \triangleq [f_{k+1}]\Big([\hat{x}_{k|k}], [u_{k+1}], [w_{k+1}]\Big),$$
$$[\hat{r}_{k+1}] \triangleq [y_{k+1}] - [h_{k+1}]\Big([\hat{x}_{k+1|k}], [u_{k+1}]\Big) - [\mu_{k+1}].$$

Then, for all $k \geq 1$:

(a) $y_k|x_k \sim \mathcal{N}(m_k, \Sigma_k)$ where $m_k = h_k(x_k, u_k) + \mu_k$ and the notation $y_k|x_k$ means for the stochastic variables y_k given (or knowing) x_k. When w_k is a bounded disturbance, then x_k is deterministic and $y_k|x_k \equiv y_k$.

(b) $r_k \sim \mathcal{N}(0, \Sigma_k)$ where $\Sigma_k \in [\Sigma_k]$.
Consequently, a *confidence interval* of (more than) 99.7% of all admissible r_k can be deduced as

$$\text{CI}(r_k) = \pm\, 3.\sqrt{\text{diag}(\overline{\Sigma}_k)},$$

with $\text{diag}(A) = (a_{11}, ..., a_{nn})^T, \forall A = (a_{ij}) \in \mathbb{R}^{n\times n}$.

Assuming further that $x_k \in [\hat{x}_{k|k}]$ at every $k \geq 1$, then:

(c) $x_{k+1} \in [\hat{x}_{k+1|k}]$ with certainty (probability 1),

(d) $r_{k+1} \in [\hat{r}_{k+1}]$ with certainty (probability 1). □

Proof. Knowing x_k in either cases of w_k (disturbance or stochastic noise), the term $h_k(x_k, u_k)$ is known (or deterministic). So, since $v_k \sim \mathcal{N}(\mu_k, \Sigma_k)$ then $y_k|x_k = h_k(x_k, u_k) + v_k$ is normally distributed with mean $m_k = h_k(x_k, u_k) + \mu_k$ and covariance Σ_k. Also, by the property of normal distribution, it concludes that $r_k \sim \mathcal{N}(0, \Sigma_k)$. So, statements (a) and (b) are proved.

To prove the statements (c) and (d), the inclusion function property is used, that is: $f(x) \in [f]([x]), \forall x \in [x]$ with certainty. By assumptions (A3) and $x_k \in [\hat{x}_{k|k}]$, then

- $f_{k+1}(x_k, u_{k+1}, w_{k+1}) = x_{k+1} \in [\hat{x}_{k+1|k}]$,
- $h_{k+1}(x_{k+1}, u_{k+1}) \in [h_{k+1}]([\hat{x}_{k+1|k}], [u_{k+1}])$,
- $\mu_{k+1} \in [\mu_{k+1}]$

with certainty. Thus, it implies that $r_{k+1} \in [\hat{r}_{k+1}]$ with certainty ensured by the inclusion function property. □

Remark 4. The notation $[\hat{x}_{k|k}]$, $k \geq 1$, denotes the interval estimate provided by the corresponding interval filter at the end of the time instant k. $[\hat{x}_{k+1|k}]$ denotes the propagation box at the next iteration that allows to obtain $[\hat{x}_{k+1|k+1}]$. □

Remark 5. The assumption $x_k \in [\hat{x}_{k|k}]$ at every $k \geq 1$ is strong and related to the performance and convergence of the filter. Practically, an interval filter that has the $O(\%) = \sum_{k=1}^{N} \mathbb{I}(x_k \in [\hat{x}_{k|k}])/N \times 100\%$ measuring the percentage of $x_k \in [\hat{x}_{k|k}]$ greater than some level (e.g. 80% or 90%) can be suited to the FD procedure of the ADFC method, although it may cause certain false alarms. □

Principle of the method

Since $r_k \sim \mathcal{N}(0, \Sigma_k)$ then $\xi_k \triangleq r_k^T \Sigma_k^{-1} r_k$ is χ^2-distributed with n_y degrees of freedom (d.f.) ($\xi_k \sim \chi^2(n_y)$). Thus, for any $a_k > 0$ so that $S_+([\Sigma_k]) \preceq a_k\, I_{n_y}$,

$$\xi_k \geq r_k^T a_k^{-1} r_k = r_k^T r_k / a_k \equiv \hat{\xi}_k.$$

However, r_k is unknown and $r_k \in [\hat{r}_k]$ with a computable $[\hat{r}_k]$. So, we aim at using the statistic

$$U_k = \sup\{\text{abs}([\hat{r}_k]^T [\hat{r}_k]/a_k)\} = \sup\{\text{abs}([\hat{\xi}_k])\}, \quad (2)$$

as proposed in Lu et al. (2021) with the a_k aforementioned. The statistic U_k is approximated by a χ^2-distributed random variable with an appropriate d.f. $\kappa_k n_y$ by determining a_k and using an a.a.c. κ_k.

Explication.

Theoretically, for ensuring $S_+([\Sigma_k]) \preceq a_k\, I_{n_y}$, it is required that $\max\{\text{diag}(\overline{\Sigma}_k)\} < a_k$ (Lu et al., 2019). The more a_k is large, the more $\hat{\xi}_k$ is small and vice versa. Besides, note that $r_k \in [\hat{r}_k]$ is with probability 1 (Theorem 3), where $r_k \sim \mathcal{N}(0, \Sigma_k)$, $\Sigma_k \in [\Sigma_k]$. This implies $[\hat{r}_k] \supset \text{CI}(r_k)$ and $[\hat{r}_k]$ must be greater considerably than the confidence interval in order to contain r_k with such a certainty. Therefore, an appropriate (optimal) a_k must ensure a compromise between $[\hat{r}_k]$ and $\text{CI}(r_k)$, says a function of $[\hat{r}_k]$ and $[\Sigma_k]$, provided that:

$$\max\{\text{diag}(\overline{\Sigma}_k)\} < a_k = \phi_k([\hat{r}_k], [\Sigma_k]) < \max\{\overline{\hat{r}_k}\}. \quad (3)$$

In the development of this section, a simple proposition for a_k is that

$$a_k = \lambda_1 \cdot \text{mean}\{\text{width}([\hat{r}_k])\} \text{ so that } S_+([\Sigma_k]) \preceq a_k I, \quad (4)$$

where $\lambda_1 > 0$ is a scaling factor changing depending on the considered application.

The a.a.c. κ_k is involved with the threshold δ_k to which U_k is compared: $\mathbb{P}\left(\chi^2(\kappa_k n_y) > \delta_k\right) = \alpha$, where α is a given *significant level*. So, $U_k \approx \chi^2(\kappa_k n_y) \leq \delta_k$ with confident level $1 - \alpha$ in the fault free case. κ_k is chosen (Lu et al., 2021) as

$$\kappa_k = \text{mean}\{\text{width}([\hat{r}_k])\}. \quad (5)$$

so that it is sensitive to the fault, large enough to obtain a small FAR (e.g. $\leq 5\%$) in the fault free case, sensitively affected by width($[\hat{r}_k]$) as well as U_k but it does not increase as fast as the later whenever a fault occurs and affects on the width($[\hat{r}_k]$). This choice also provided a good performance fault detection with FAR $< 3\%$ in several scenarios of simulations presented in the referenced paper. Thus, in the present work, it is raised naturally that

$$\kappa_k \;=\; \lambda_2 \cdot \text{mean}\{\text{width}([\hat{r}_k])\} \tag{6}$$

is chosen for adapting to different applications and purposes by using different *level parameters* $\lambda_2 > 0$.

Thanks to the use of RLBPF with interval analysis properties, the enlarged method is provided without assumptions about dynamic functions f_k and h_k nor any linearization is required.

Remark 6. In linear systems, residuals are determined by $r_k = y_k - h_k(\hat{x}_k, u_k) - \mu_k$ where $\hat{x}_k$ is an estimate of x_k and h_k is a linear function. Thus, r_k can be computed explicitly at every time step as well as its distribution under the SKF assumptions. Consequently, with additional bounded uncertainties, the covariance of $[r_k]$ is well determined as some computable matrix $[\Sigma_k]$ and a_k has a more accurate choice using Theorem 2 in Lu et al. (2021) so that $S_+([\Sigma_k]) \preceq a_k I_{n_y}$. Evidently, if $[\Sigma_k]$ is assumed to be known in assumption (A4), a_k can be computed in the same manner. In this work, we consider $r_k = y_k - h_k(x_k, u_k) - \mu_k$, although it is unknown, and compute $[\hat{r}_k]$ ensuring that $r_k \in [\hat{r}_k]$ with certainty. □

The ADFC method is eventually enlarged to a more general framework of non linear system, as presented above. It can be summarized by the following algorithm.

Algorithm 1 ADFC method to nonlinear system

Initialization: α, λ_1, λ_2, $[\hat{x}_{0|0}] \equiv [x_0], f_k, h_k$, $[u_k]$, $[w_k]$, $[y_k]$, $[\mu_k]$, $[\Sigma_k]$, $k = 1, 2, ..., N$.
for $k = 1, 2, 3, ...N$ **do**
  Use RLBPF to get: $[\hat{x}_{k-1|k-1}]$
  $[\hat{x}_{k|k-1}] = [f_k]([\hat{x}_{k-1|k-1}], [u_k], [w_k])$
  $[\hat{r}_k] = [y_k] - [h_k]([\hat{x}_{k|k-1}], [u_k]) - [\mu_k]$
  $a_k = \lambda_1 \cdot \text{mean}\{\text{width}([\hat{r}_k])\}$
  $U_k = \sup\{\text{abs}([\hat{r}_k]^T [\hat{r}_k]/a_k)\}$
  $\kappa_k = \lambda_2 \cdot \text{mean}\{\text{width}([\hat{r}_k])\}$
  Find δ_k s.t.: $\mathbb{P}(\chi^2(\kappa_k n_y) > \delta_k) = \alpha$.
  Detection signal : $\pi_k = \mathbb{I}(U_k > \delta_k)$.
end for

4. APPLICATION

4.1 Quarter vehicle model

The vertical quarter car model is often used to study the vertical behavior of a vehicle according to the suspension characteristic (passive or controlled) (Fig. 2). When controlled suspension is considered, the passive damper F_c is removed and replaced by an actuator that provides a force u either active or semi-active depending on the chosen actuator (Fig. 3). In figures 2, the sprung mass m_s and unsprung mass m_{us} represent respectively the vehicle chassis and the vehicle wheel. z_s and z_{us} are respectively the relative vertical displacement of the vehicle chassis and the vehicle wheel with respect to the road. z_r is considered as the road disturbance.

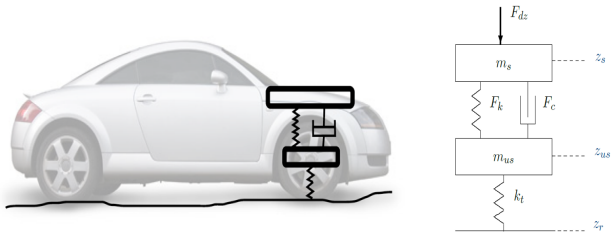

Fig. 2. Quarter vehicle model

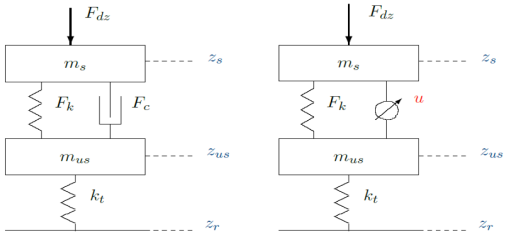

Fig. 3. Quarter vehical model - Passive (left) and Active control (right) modes

Vertical efforts generated by the suspension and tire elements are nonlinear. Let recall that:

$$\begin{cases} F_{tz} \;=\; k_t\,(z_{us} - z_r) \;+\; c_t\,(\dot{z}_{us} - \dot{z}_r) & \\ F_{sz} \;=\; F_k\,(z_s - z_{us}) \;+\; F_c\,(\dot{z}_s - \dot{z}_{us}) & \text{(passive suspension)} \\ F_{sz} \;=\; F_k\,(z_s - z_{us}) \;+\; \quad u \quad & \text{(controlled suspension)} \end{cases} \tag{7}$$

where k_t and c_t are the linear tire stiffness and damping factors, F_{tz} the tire force usually assumed to be linear and F_{sz} the suspension force.
The vertical quarter car model is given by the following dynamical equations,

$$\begin{cases} m_s \ddot{z}_s \;=\; -\,(F_{sz} + F_{dz}) \\ m_{us} \ddot{z}_{us} \;=\; F_{sz} - F_{tz} \end{cases} \tag{8}$$

where

- $z_{def} = (z_s - z_{us})$ is the suspension deflection,
- z_s and z_{us} are the chassis and unsprung masses bounce,
- m_s and m_{us} are sprung and unsprung masses,
- $F_k(.)$ is a nonlinear function of z_{def},
- $F_c(.)$ is a nonlinear function of $\dot{z}_{def}$,
- F_{dz} describes a vertical disturbance force (that can be caused by a load transfer, e.g. steering situation).

Then, according to the suspension model chosen, different kinds of quarter car models may be obtained:

- If $u = F_c(\dot{z}_{def})$, the suspension is passive.
- If $u = F_c(\dot{z}_{def}, \Omega)$, the suspension is semi-active, where Ω is input parameter of the controlled damper that modifies the damping factor.
- If u is an independent function, the quarter car is said to be active.

Remark 7. In the vertical quarter vehicle model, the nonlinear phenomena come from the force description of the suspension elements and not from the equation structure. Therefore, the model can be set as a LPV system.
The unsprung mass m_{us} corresponds to the set of elements that compose the wheel, the suspension system and multiple links from the chassis to the"road". Without loss of

generality, it is often referred to as the wheel since z_{us} is the center of the wheel. □

4.2 Simulation

Consider the following nonlinear system modeling the MR (Magneto-Rheological) damper:

$$\begin{cases} m_s\ddot{z}_s &= -k_s z_{def} - F_{damper} \\ m_{us}\ddot{z}_{us} &= k_s z_{def} + F_{damper} - k_t(z_{us} - z_r) \end{cases}, \quad (9)$$

$$F_{damper} = c_0\dot{z}_{def} + k_0 z_{def} + f_I \tanh\left(c_1\dot{z}_{def} + k_1 z_{def}\right),$$

where c_0, k_0, c_1, k_1 are constant chosen according to (Nino-Juarez et al., 2008) such that

$$c_0 = 1500\ (\mathrm{Nsm}^{-1}), \qquad c_1 = 129\ (\mathrm{sm}^{-1}),$$
$$k_0 = 989\ (\mathrm{Nm}^{-1}), \qquad k_1 = 85\ (\mathrm{m}^{-1}),$$

and f_I is a controllable force depending on the input current I and satisfying the dissipativity constraint

$$0 < f_{\min} \leq f_I \leq f_{\max}.$$

In this simulation, we consider $f_{\min} = 1000$ N/m and $f_{\max} = 1500$ N/m. Other parameter values used in the simulation are presented in Table 1 issued from (Fergani, 2014).

Symbol	Value	Unit	Signification
m_s	315	kg	sprung mass
m_{us}	37.5	kg	unsprung mass
k_s	29500	N/m	suspension linearized stiffness
k_t	208000	N/m	tire stiffness
z_{def}	$[-0.09; 0.05]$	m	suspension bound (stroke limit)

Table 1. Linearized Renault Mégane Coupé parameters of the quarter vertical model (front suspension).

Comparing to the general system (8), in the MR damper model (9), assume that $F_{dz} = 0$ and $F_{tz} = k_t(z_{us} - z_r)$.

Putting

- $x = [z_s, \dot{z}_s, z_{us}, \dot{z}_{us}]^T$ as state variable under consideration and $x(i)$, $i \in \{1, ..., 4\}$, are its components,
- $u = f_I$ as controllable input,
- $w = z_r$,

then x, u, w are functions of time t and the state-space representation of (9) is expressed in the form

$$\dot{x}_t = f(t, x_t) = \begin{bmatrix} f_1(t, x_t) \\ f_2(t, x_t) \\ f_3(t, x_t) \\ f_4(t, x_t) \end{bmatrix}, \quad (10)$$

where

$$\begin{aligned} f_1(t, x_t) &= e_2^T x_t \\ f_3(t, x_t) &= e_4^T x_t \\ f_2(t, x_t) &= \left(a^T x_t - u_t \tanh(b^T x_t)\right)/m_s \\ f_4(t, x_t) &= \left(c^T x_t + u_t \tanh(b^T x_t) + k_t w_t\right)/m_{us} \end{aligned},$$

with e_i's are i-th column vectors of the corresponding identity matrix and

$$a = \begin{bmatrix} -k_s - k_0 \\ -c_0 \\ k_s + k_0 \\ c_0 \end{bmatrix}, \quad b = \begin{bmatrix} k_1 \\ c_1 \\ -k_1 \\ -c_1 \end{bmatrix}, \quad c = \begin{bmatrix} k_s + k_0 \\ c_0 \\ -k_s - k_0 - k_t \\ -c_0 \end{bmatrix}.$$

The system (10) will be discretized using the Fourth order Runge-Kutta method (Kincaid and Cheney, 1991) with a chosen sampling time $T = 10^{-4}$(s). The resulted discrete time state dynamical system is denoted by:

$$x_k = \tilde{f}(x_{k-1}, u_k, w_k) + \eta_k, \qquad k \in \mathbb{N}^*, \quad (11)$$

where η_k is assumed to be Gaussian noise with zero mean and covariances $10^{-8} I_{n_x}$. The corresponding observed measurements are assumed to be z_{def} at every time step, thus the measurement dynamical equation can be expressed in the form

$$y_k = h(x_k) + v_k = Cx_k + v_k, C = [1, 0, -1, 0] \quad (12)$$

where v_k is assumed to be Gaussian with mean $\mu_k \in [\mu_k] = [-0.005, 0.005]$ and variance $\sigma_k^2 \in [\sigma_k^2] = [1, 4] * 10^{-6}$. The precision of the sensors is assumed to be ± 0.005 (m).

State and measurement simulation: Assume that the initial state is $x_0 = (0, 0, 0, 0)^T$, the control force input is set to get its maximum value constantly ($u = 1500$) for all time instants and the road disturbance is set as $w = 0.05 \max\{0, \sin(\pi t)\}$. $\{x_k, y_k\}_{k=1:N}$ are then generated using (11) and (12) for $N = 5000$ steps. The measurements obtained will be intervals $[y_k] = y_k \pm 0.005$ because of sensor errors.

For the fault detection purpose, a fault of an amplitude of $b = 0.02$m is added to the simulated observed measurements in a range $\mathcal{R}$ with length $l = 200$ and the following choices are used: $\lambda_1 = 0.02$, $\lambda_2 = 10$, $\alpha = 0.03$.

A simulation result is figured out in Figures 4 - 6. In the error range, the residual deviate from 0 (Fig. 4) and most of the statistics U_k (blue line) passe over the adaptive thresholds δ_k (red line) (Fig. 5).

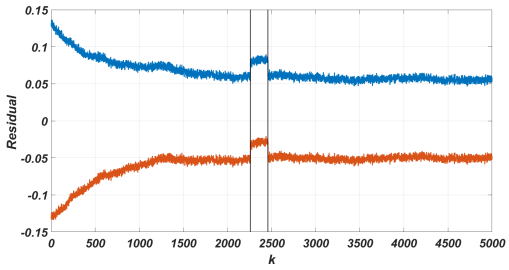

Fig. 4. ADFC method - Residual $[\hat{r}_k]$ for a Quarter vehicle model with sensor fault.

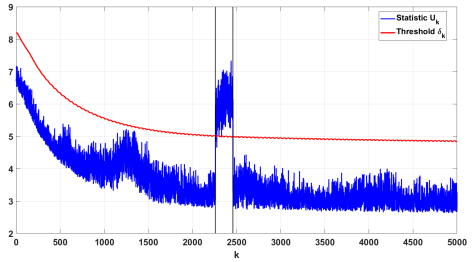

Fig. 5. ADFC method - Fault detection to a Quarter vehicle model.

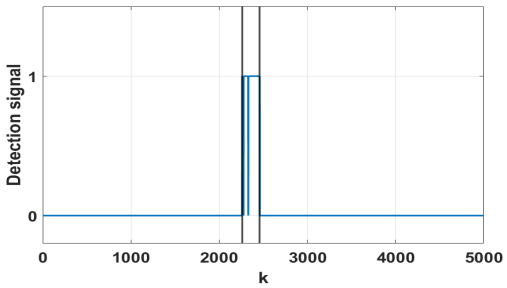

Fig. 6. ADFC method - Detection signal for a Quarter vehicle model.

Then the fault detection procedure is replicated for $L = 100$ times where the error range $\mathcal{R}$ is chosen randomly and indicators DR, NDR, FAR, EFF are yielded as their corresponding means after L times of simulations (Table 2). For a fault value $b = 0.02$m, the efficiency index (EFF) is about 66%.

b	DR(%)	NDR(%)	FAR(%)	EFF (%)
0.02	67.715	32.285	1.2762	66.439

Table 2. ADFC method - Fault detection to a Quarter vehicle model.

5. CONCLUSION AND PERSPECTIVE

An adaptive approach of sensor fault detection applied to nonlinear discrete time dynamical system is proposed. The approach combines RLBPF with a hypothesis testing method using χ^2-statistics with adaptive degrees of freedom. Theoretical framework is developed thanks to interval analysis. A great flexibility of adjusting several factors (parameters) makes the approach highly fitted to multiple applications.

Simulations are performed using the nonlinear Magneto-Rheological damper model. The results show the efficiency of the proposed method providing good performances w.r.t the fault magnitudes.

The method is developed however in the framework of (additive) sensor fault systems. Extend this method to deal with other kinds of fault (e.g. actuator faults) and with fault identification is a perspective of our future research.

REFERENCES

Chevet, T., Dinh, T.N., Marzat, J., and Raïssi, T. (2021). Robust sensor fault detection for linear parameter-varying systems using interval observer. In *Proceedings of the 31th European Safety and Reliability Conference*. doi:https://doi.org/10.3850/981-973-0000-00-0esrel2021. URL `https://www.sciencedirect.com/science/article/pii/S0925231218304715`.

Fergani, S. (2014). *Robust multivariable control for vehicle dynamics*. PhD thesis, Grenoble INP, GIPSA-lab, Control System dpt., Grenoble, France.

Jaulin, L., Kieffer, M., Didrit, O., and Walter, E. (2001). *Applied Interval Analysis, with Examples in Parameter and State Estimation, Robust Control and Robotics*. Springer-Verlag, London.

Kalman, R. (1960). A new approach to linear filtering and prediction problems. *Transactions of the ASME–Journal of Basic Engineering*, 82(Series D), 35–45.

Kincaid, D. and Cheney, W. (1991). *Numerical Analysis*. Brooks/Cole Publishing Company, Wadsworth, Inc.

Lu, Q.H., Fergani, S., and Jauberthie, C. (2021). A new scheme for fault detection based on Optimal Upper Bounded Interval Kalman Filter. *IFAC-PapersOnLine*, 54(7), 292–297. doi:https://doi.org/10.1016/j.ifacol.2021.08.374. URL `https://www.sciencedirect.com/science/article/pii/S2405896321011484`. 19th IFAC Symposium on System Identification SYSID 2021.

Lu, Q.H., Fergani, S., and Jauberthie, C. (2022). Reinforced likelihood box particle filter. *IEEE Control Systems Letters*, 7, 502–507. doi:10.1109/LCSYS.2022.3194810.

Lu, Q.H., Fergani, S., Jauberthie, C., and Le Gall, F. (2019). Optimally bounded interval kalman filter. In *2019 IEEE 58th Conference on Decision and Control (CDC)*, 379–384. doi:10.1109/CDC40024.2019.9028918.

Mohamadi, L., Dai, X., Busawon, K., and Djemai, M. (2016). Output observer for fault detection in linear systems. In *2016 IEEE 14th International Conference on Industrial Informatics (INDIN)*, 1262–1267. doi:10.1109/INDIN.2016.7819361.

Nino-Juarez, E., Ramirez-Mendoza, R., Morales-Menendez, R., Sename, O., and Dugard, L. (2008). Minimizing the frequency effect in a black box model of a magneto-rheological damper. In *Mini conference; 11th, Vehicle system dynamics, identification and anomalies*, 733–742. Technical University of Budapest.

Puig, V. (2010). Fault diagnosis and fault tolerant control using set-membership approaches: Application to real case studies. *International Journal of Applied Mathematics and Computer Science*, 20(4), 619–635.

Raka, S.A. and Combastel, C. (2013). Fault detection based on robust adaptive thresholds: A dynamic interval approach. *Annual Reviews in Control*, 37(1), 119–128.

Rump, S. (1999). INTLAB - INTerval LABoratory. In T. Csendes (ed.), *Developments in Reliable Computing*, 77–104. Kluwer Academic Publishers, Dordrecht. `http://www.tuhh.de/ti3/rump/`.

Tran, T. (2017). *Cadre unifié pour la modélisation des incertitudes statistiques et bornées - Application à la détection et isolation de défauts dans les systèmes dynamiques incertains par estimation*. Phd thesis, EDSYS, Université Toulouse III Paul Sabatier, LAAS-lab, Toulouse, France.

Xiong, J., Jauberthie, C., Travé-Massuyès, L., and Le Gall, F. (2013). Fault detection using interval Kalman filtering enhanced by constraint propagation. In *Proceedings of the 52nd IEEE Annual Conference on Decision and Control (CDC)*, 490–495. Florence, Italy.

Zhong, M., Xue, T., and Ding, S.X. (2018). A survey on model-based fault diagnosis for linear discrete time-varying systems. *Neurocomputing*, 306, 51–60. doi:https://doi.org/10.1016/j.neucom.2018.04.037. URL `https://www.sciencedirect.com/science/article/pii/S0925231218304715`.